35th Annual International Conference of the IEEE EMBS
Osaka, Japan, 3 - 7 July, 2013

Energy Back-projective Composition for 3-D Coronary Artery Reconstruction*

Weijian Cong, Jian Yang*, Yue Liu, Yongtian Wang

Abstract—**This paper presents a novel energy back-projective composition model (EBPCM) for 3-D reconstruction of the coronary arteries from two mono-plane angiographic images. A major problem with the commonly used parameter deformable model is that the predefined correspondences may become non-strict matching after the curve evolution, which generally leads to large extra calculation errors. In this study, the energy field in the image is back-projected to 3-D space and decomposed into three independent components in the world coordinates centered at the iso-center of the C-arm. Then, the components from different views are composited together according to the rotation and scaling relationship of the imaging angles. The composited energy field hence is utilized as the external force to control the evolution of the vascular structure in 3-D space. As the driving force is iteratively updated according to energy in the two projection images, the non-strict matching can be effectively avoided. Also, the proposed method is very flexible, which can be composited with any energy fields such as Generalized Gradient Vector Flow (GGVF) and Potential Energy (PE) etc. Experiments demonstrate that the proposed method is very effective and robust, when using GGVF as the external force, the reconstruction RMS error can be reduced to about 0.595mm in the 3-D space.**

I. Introduction

X-ray angiography (XRA) is a powerful technique to visualize vasculature, which has been widely used for cardiac diseases diagnosis and interventional treatment. Besides that, XRA has been regarded as the golden standard for the diagnosis of coronary artery diseases. However, as XRA image is the perspective projection of anatomic structures from 3-D space using X-ray, much 3-D information about the coronary arteries may be lost in the process. The successful diagnosis of related diseases usually requires profound professional knowledge and operation experience. 3-D reconstruction of coronary arteries not only can provide the physician with clear vascular structure in 3-D space, but also can supply quantitative information of vasculature, including diameter, length, perfusion volume and optimum imaging angle, etc. Hence, 3-D reconstruction technique has important clinical values in the diagnosis of vascular related disease [1].

Current 3-D reconstruction method of coronary arteries can be classified into two main categories: bottom-up and top-down method. For the bottom-up method, correspondence determination is the key procedure for which feature matching procedure is usually constructed by epipolar geometry theory [2,3] and the accuracy of 3-D reconstruction is strictly correlated with the correspondence results. One critical problem is that it is difficult to find the true correspondence, especially when the vessel segment is overlapped or is parallel with the epipolar line. Hence, large errors may be introduced during the 3-D reconstruction. For the top-down method, vessel segment is generally constructed as parameterized deformation model which evolves under the constraints of the combination of internal and external energies in the 2-D projection images [4-6]. As a result, the vascular structure in 3-D space deforms to adapt its structure to a stable representation, which has minimum projection errors in all of the projections. This method avoids the calculation of correspondences and therefore, is much more flexible than the bottom-up method.

In this paper, a novel deformable model is proposed for the 3-D reconstruction of the coronary arteries from two angiographic images. Different from the traditional snake deformable model in which the curve is deformed in the projection images, the 3-D curve evolves in 3-D space according to the energy composition from the two 2-D projections. The proposed method is described as follows. Firstly, relative transformation, including rotation and translation between two angiographic images, is constructed based on the projection parameters, including the image head files. A straight line is then parameterized in 3-D space, which is constructed by two pairs of correspondence in angiographic views by geometrical triangulation method. Thereafter , the straight line is projected into the two angiographic views and the energy fields at every sampling point on the projection line are calculated. Then, the energy fields in the 2-D angiographic images are back-projected to the 3-D space and composited in the same coordinate system, which can be used as the pushing forces for the evolution of the deformable curve. In this study, the proposed energy back-projection and composition is called Energy Back-projective Composition Model (EBPCM). Elasticity and bending forces are employed and integrated as internal energy to preserve the smoothness and topology of the deformation curve. Under the combination of constructed internal and external energies, the predefined straight line evolves iteratively in the 3-D space toward the true representation of the vascular structures. The projections of the curve under iterations in the 2-D angiographic images will also deform gradually toward the vascular branches, which helps in effectively avoiding the correspondence matching problem.

*This research was supported by the National Basic Research Program of China (2010CB732505), New Century Excellent Talents in University of Ministry of Education of China (NCET-10-0049) and the Plan of Excellent Talent in Beijing (2010D009011000004).

Weijing Cong, Jian Yang*, Yue Liu and Yongtian Wang are with Key Laboratory of Photoelectronic Imaging Technology and System, Ministry of Education of China, School of Optics and Electronics, Beijing Institute of Technology, Beijing 100081, China. (*corresponding author: jyang@bit.edu.cn)

II. DEFORMATION MODEL BASED 3D RECONSTRUCTION METHOD

A. Deformable model of open curve

Suppose an open 3-D curve is $X(s)=[x(s),y(s),z(s)], s\in[0,1]$, then the parameter deformation model can be generally defined as

$$E_{energy}=\int_0^1 [E_{internal}(X(s))+E_{external}(X(s))]ds\ , \qquad (1)$$

Where $E_{internal}$ and $E_{external}$ are internal and external energies, respectively. For a deformable curve, the external energy pushes the curve to deform its shape, while the internal energy serves to maintain its smoothness. Up till now, various external energies such as Gaussian energy, balloon model, Potential Energy, Gradient Vector Flow (GVF) and Generalized Gradient Vector Flow (GGVF)[7] etc. have been proposed by numerous researchers. In this study, GGVF proposed by Xu *et al*. in 1998 is utilized to serve as the external driving energy. The following section will provide a general introduction to GGVF.

The edge map of the image may be defined as $f(u,v)$, and the energy of the vector field is $E_{image}(u,v)=[eu(u,v),ev(u,v)]$, where $eu(u,v)$ and $ev(u,v)$ are gradient vectors at point (u,v) in the horizontal and vertical directions, respectively. In such a case, the energy function is represented by:

$$\varepsilon=\iint \mu(eu_u^2+eu_v^2+ev_u^2+ev_v^2)+|\nabla f|^2|E_{image}-\nabla f|^2\ dudv\ . \qquad (2)$$

Where eu_u and ev_u are the first derivative of eu and ev with respect to direction u, whereas eu_v and ev_v are the first derivative with respect to direction v.

B. Energy Back-projective Composition Model (EBPCM)

The former top-down methods for 3-D reconstruction of vascular structures from angiographic images generally employed parameter deformation models for the curve deformation, as can be found in [4-6]. For this method, every step of iteration strictly depends on the two energies in the two 2-D images, and the motion vectors of each correspondence pair need to be recorded so that the 3-D vessel can be reconstructed. From our research, we found that during the curve deforming, the correspondences in two images no longer satisfy the widely used epipolar constraints. If the 3-D vessel is reconstructed by the wrong correspondences, error may gradually accumulate during the iteration process and this problem was identified in the next experimental section.

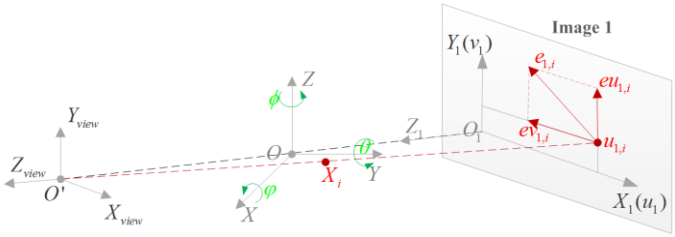

Figure 1. Energy back-projection and scaling principle.

To solve this problem, the energies in the images are back-projected to the 3-D space, as can be seen in Fig.1. We construct 3-D coordinates $O_j-X_jY_jZ_j$ at the optical center of the j*th* image, for which X_j and Y_j are parallel to the image coordinates u_j and v_j, respectively. Then, on the basis of left hand rule, the direction of Z_j can be obtained by calculating the cross product of X_j and Y_j. Let φ, θ and ϕ denote the rotation angles between coordinates $O_j-X_jY_jZ_j$ and the original coordinates $O-XYZ$ correspond to x, y and z axis respectively. Let $eu_{j,i}$ and $ev_{j,i}$ represent the back-projected energy corresponding to the axis of u_j and v_j respectively. In this study, the rotation order is defined as $X\to Y\to Z$.

As composition and subtraction of space vectors are only decided by their rotation angles, the effect of translation can be neglected for the energy composition. Then, the two components $eu_{j,i}$ and $ev_{j,i}$ of the external energy are back-projected into 3-D space and decomposed into the three axis of the $O-XYZ$, which can be defined as follows:

$$\begin{cases} ex_{j,i}=eu_{j,i}\cos(\phi_j)\cos(\theta_j)-ev_{j,i}\sin(\phi_j)\cos(\theta_j) \\ ey_{j,i}=eu_{j,i}\cos(\phi_j)\sin(\theta_j)\sin(\varphi_j)+eu_{j,i}\sin(\phi_j)\cos(\varphi_j) \\ \quad +ev_{j,i}\cos(\phi_j)\cos(\varphi_j)-ev_{j,i}\sin(\phi_j)\sin(\theta_j)\sin(\varphi_j)\ . \\ ez_{j,i}=-eu_{j,i}\cos(\phi_j)\sin(\theta_j)\cos(\varphi_j)+eu_{j,i}\sin(\phi_j)\sin(\varphi_j) \\ \quad +ev_{j,i}\cos(\phi_j)\sin(\varphi_j)-ev_{j,i}\sin(\phi_j)\sin(\theta_j)\cos(\varphi_j) \end{cases} \qquad (3)$$

Where $ex_{j,i}$, $ey_{j,i}$ and $ez_{j,i}$ are the energy components along the three axis.

As the energy components from different angiographic images are independent and can be composited together. Hence, for multiple views we have:

$$\begin{cases} ex_{j,i}^{sum}=\sum_{j=1}^{m} ex_{j,i}\cos(\phi_{j,i})\cos(\theta_{j,i})+\sum_{j=1}^{m} ey_{j,i}\sin(\phi_{j,i})\cos(\theta_{j,i}) \\ ey_{j,i}^{sum}=\sum_{j=1}^{m} ex_{j,i}\cos(\phi_{j,i})\sin(\theta_{j,i})\sin(\varphi_{j,i})+\sum_{j=1}^{m} ex_{j,i}\sin(\phi_{j,i})\cos(\varphi_{j,i}) \\ \quad +\sum_{j=1}^{m} ey_{j,i}\cos(\phi_{j,i})\cos(\varphi_{j,i})-\sum_{j=1}^{m} ey_{j,i}\sin(\phi_{j,i})\sin(\theta_{j,i})\sin(\varphi_{j,i})\ . \\ ez_{j,i}^{sum}=-\sum_{j=1}^{m} ex_{j,i}\cos(\phi_{j,i})\sin(\theta_{j,i})\cos(\varphi_{j,i})+\sum_{j=1}^{m} ex_{j,i}\sin(\phi_{j,i})\sin(\varphi_{j,i}) \\ \quad +\sum_{j=1}^{m} ey_{j,i}\cos(\phi_{j,i})\sin(\varphi_{j,i})-\sum_{j=1}^{m} ey_{j,i}\sin(\phi_{j,i})\sin(\theta_{j,i})\cos(\varphi_{j,i}) \end{cases} \qquad (4)$$

Where m denotes the number of views, while $ex_{j,i}^{sum}$, $ey_{j,i}^{sum}$ and $ez_{j,i}^{sum}$ represent the summaries of energy component in the three axis in coordinate $O-XYZ$.

Under the composited energies of internal and external constraint in 3-D space, all the points on the predefined curve can evolve gradually to adapt the shape of the curve to the condition that the total re-projection errors will reach the minimum. The developed energy back-projection and composition model is very general and can be used for any form of external energy such as PE, GVF and GGVF. In addition, the model is not only limited to two angiographic images, but can also be utilized for multiple views. In this study, all the three above mentioned energies are tested in the experimental parts.

TABLE I. COMPARISON OF RECONSTRUCTION RESULTS FOR DIFFERENT ALGORITHMS FOR FOUR SIMULATED IMAGE PAIRS.

Data	Images	Initial	EPIM				EBPCM			
			PE		*GGVF*		*PE*		*GGVF*	
		RMS(mm)	*RMS(mm)*	$\frac{\delta_0-\delta}{\delta_0}$	*RMS(mm)*	$\frac{\delta_0-\delta}{\delta_0}$	*RMS(mm)*	$\frac{\delta_0-\delta}{\delta_0}$	*RMS(mm)*	$\frac{\delta_0-\delta}{\delta_0}$
1	IRPE 1	5.164	0.396	92.33%	0.466	90.98%	0.379	92.65%	0.409	92.08%
	IRPE 2	5.592	0.418	92.52%	0.434	92.25%	0.453	91.90%	0.411	92.64%
	SE	5.845	1.243	78.73%	0.597	89.79%	1.056	81.94%	0.682	88.33%
2	IRPE 1	6.184	0.393	93.64%	0.377	93.91%	0.360	94.17%	0.449	92.75%
	IRPE 2	6.542	0.374	94.28%	0.471	92.79%	0.426	93.49%	0.327	95.00%
	SE	6.734	1.344	80.05%	0.711	89.45%	1.121	83.36%	0.637	90.54%
3	IRPE 1	7.162	0.408	94.31%	0.428	94.02%	0.403	94.37%	0.418	94.16%
	IRPE 2	6.637	0.413	93.78%	0.395	94.05%	0.417	93.72%	0.407	93.87%
	SE	6.195	1.065	82.81%	0.684	88.96%	1.026	83.44%	0.544	91.22%
4	IRPE 1	5.394	0.398	92.63%	0.414	92.33%	0.372	93.10%	0.408	92.45%
	IRPE 2	5.955	0.346	94.18%	0.401	93.26%	0.399	93.29%	0.404	93.22%
	SE	5.961	1.045	82.46%	0.663	88.88%	0.914	84.67%	0.515	91.36%
AVG	IRPE	6.079	0.393	93.46%	0.423	92.95%	0.401	93.34%	0.404	93.27%
	SE	6.184	1.174	81.01%	0.664	89.27%	1.029	83.35%	0.595	90.36%

III. EXPERIMENTAL RESULTS

In order to investigate the performance of the proposed method, a series of experiments are tested on phantom data and routine clinical angiograms. The phantom data is simulated from CTA data obtained from MACCAI Grand Challenge 2012, while the routine angiographic images are obtained from a GE Innva 2000 XRA device at Beijing Anzhen Hospital. The criterion to quantify the accuracy is taken as two folds: (1) Image re-projection error (IRPE): the Euclidean distance between a set of centerline points in projection image and the corresponding re-projected 2-D centerline points in the image; (2) Space error (SE): the Euclidean distance between a set of centerline points of the phantom data and the reconstructed centerline points in 3-D space. Let δ_0 and δ represent the initial and the reconstructed RMS errors, by calculating the RMS reduction ratio $\frac{\delta_0-\delta}{\delta_0}$, the performance of the evaluating method can be effectively quantified.

A. Phantom data

As we have mentioned in this paper, the point-to-point corresponding relationship will be transformed continuously with the deformation of the curve in the projection images. In order to investigate the non-strict matching problem, the motion trajectories of the curves are recorded at each iteration. So how the deformation model affects the epipolar geometry can be effectively quantified. Fig. 2(A) and 2(B) give the two image planes. 2(A1) and 2(B1) are the corresponding deformation curves in 3-D space. The blue and green curves represent the locations of the deformation curve at the first and the second iteration respectively. The red curves represent the true vascular centerline, while the light-blue straight lines in the second column represent the epipolar lines corresponding to points u_1^1 and u_1^2 in first view. Initially, u_1^1 and u_2^2 are point pairs strictly satisfying epipolar constraint. After one step of iteration, u_1^1 and u_1^2 are no longer accord with the epipolar geometry, there is an offset d between the epipolar line intersection and the point u_2^2. Hence, if the space point is directly reconstructed from u_1^2 and u_1^2, large error must be involved in the reconstruction process.

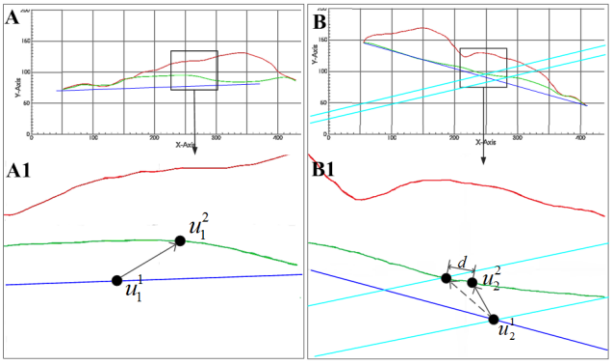

Figure 2. Non-strict matching during two steps of iterations.

In order to solve the non-strict matching problem, the EBPCM is proposed for deforming the vascular centerline, and hence, improving the reconstruction accuracy. To evaluate the performance of the proposed method, in this part, the traditional widely used Energy Projection and Iteration model (EPIM) is realized and compared with the developed EBPCM. Both the EBPCM and EPIM can utilize different forms of external energies, including PE and GGVF. Hence, the two models and three energies are composited and realized to form four types of methods. Fig. 3 shows reconstruction SE at every iteration step for the four methods. The upper figure shows calculation errors on every iteration step, while the lower figure gives magnified view of the last five iterations. From the upper figure, it can be seen that the proposed EBPCM based methods converge more rapidly than the EPIM based methods. From the lower figure, it can be seen that, the EBPCM based method can obtain high reconstruction accuracy than the EPIM based method.

Table I lists the final reconstruction results of different algorithms. It can be observed that the proposed EBRCM based method is better than the traditional EPIM based method for all the three types of external energies, the comparatively increasing ratios are 2.34% and 1.09% for PE and GGVF, respectively. For all the image pairs tested, the GGVF EBPCM based method outperforms the other

algorithms, which can achieve the best 3-D reconstruction error of 0.553mm. Obviously, the proposed GGVF EBPCM method is very effective for the vascular reconstruction from two projection images.

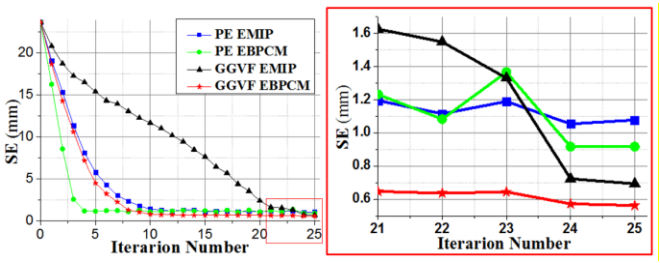

Figure 3. Space error for the four methods at every iteration steps.

B. *Clinical coronary angiogram*

From the above experiments, different algorithms are validated on phantom data sets. It can be concluded that the proposed GGVF EBPCM based method is very effective and can obtain the best reconstruction accuracy. Hence, in this part, the GGVF EBPCM based method is utilized to reconstruct the whole vascular structures. In order to reduce the cardiac motion interference and obtain the same cardiac phase, Electrocardiograph gating is used in the acquisition procedures. Table II lists the IRPE of the proposed GGVF EBPCM based method. As seen from the table, the image re-projection errors are reduced compared to the original errors. The mean RMS error is reduced from 6.739mm to 0.411mm for the proposed GGVF EBPCM based method over the 5 data sets.

TABLE II. ERROR STATISTICS OF EUCLIDEAN DISTANCES BETWEEN THE EXTRACTED CENTERLINE POINTS AND CORRESPONDING RE-PROJECTIONS OF THE RECONSTRUCTED 3-D CENTERLINE POINTS IN THE TWO VIEWS.

Data	Images	Initial RMS (mm)	GGVF EBPCM RMS (mm)
1	IRPE 1	6.622	0.402
	IRPE 2	7.314	0.377
2	IRPE 1	7.272	0.406
	IRPE 2	6.854	0.452
3	IRPE 1	6.388	0.384
	IRPE 2	6.367	0.414
4	IRPE 1	6.837	0.453
	IRPE 2	6.735	0.403
AVERAGE		6.739	0.411

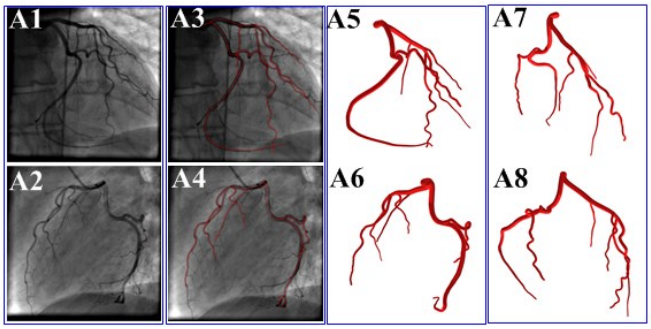

Figure 4. Final reconstruction results of data set 1.

Fig.4 gives the final reconstruction results of data 1 in Table II. 4(A3) and 4(A4) are the re-projections of the reconstructed model superposed on the corresponding views. 4(A5) and 4(A6) show the reconstructed 3-D model of the coronary arteries at the two corresponding view angles. It can be seen that the reconstructed model of the coronary arteries are perfectly matched with the vasculatures in the two angiograms, and few differences can be found in the corresponding views. Real coronary arteries are obtained, and the hidden parts are clearly recovered.

IV. CONCLUSION AND DISCUSSION

In this paper, a novel deformable model based method is proposed for reconstructing coronary arteries from a pair of monoplane angiographic images. With regards to the error accumulation problem attributed to the non-strict matching for the deformable model, a novel energy back-projective composition model (EBPCM) with GGVF is improved to determine the external energyand two models with three commonly used energies are utilized and compared. Experimental results on phantom data and clinical angiographic images demonstrate that the proposed reconstruction method is very effective and robust for the reconstruction of the coronary arteries from two mono-plane angiographic images. The re-projection error of the reconstructed skeletons in angiographic images is less than 0.45mm, while the reconstruction error in 3-D space is less than 0.60mm. From the experiments, it can be seen that realistic coronary artery trees can be recovered from different angiographic images, and hidden parts can be clearly visualized.

REFERENCES

[1] A. Wahle, J. J. Lopez, M. E. Olszewski et al., "Plaque development, vessel curvature, and wall shear stress in coronary arteries assessed by X-ray angiography and intravascular ultrasound," *Medical Image Analysis*, 2006, vol. 10, no. 4, pp. 615-631.

[2] J. Yang, Y. Wang, Y. Liu *et al.*, "Novel approach for 3-D reconstruction of coronary arteries from two uncalibrated angiographic images," *IEEE Trans. Image Processing,* 2009, vol. 18, no. 7, pp. 1563-1572.

[3] R. Liao, D. Luc, Y. Sun et al., "3-D reconstruction of the coronary artery tree from multiple views of a rotational X-ray angiography," *The International Journal of Cardiovascular Imaging (formerly Cardiac Imaging)*, 2010, vol. 26, no. 7, pp. 733-749.

[4] C. Molina, G. Prause, P. Radeva et al., "3-D catheter path reconstruction from biplane angiograms," *Proc. Medical Imaging*, 1998, pp. 504-512.

[5] C. Cañero, F. Vilariño, J. Mauri et al., "Predictive (un) distortion model and 3-D reconstruction by biplane snakes," *IEEE Trans. Medical Imaging*, 2002, vol. 21, no. 9, pp. 1188-1201.

[6] S. Zheng, T. Meiying, and S. Jian, "Sequential reconstruction of vessel skeletons from X-ray coronary angiographic sequences," *Computerized Medical Imaging and Graphics*, 2010, vol. 34, no. 5, pp. 333-345.

[7] C. Xu, and J. L. Prince, "Generalized gradient vector flow external forces for active contours," *Signal Processing*, 1998, vol. 71, no. 2, pp. 131-139.